

## Magnetic flux oscillations in partially irradiated $\text{Bi}_2\text{Sr}_2\text{CaCu}_2\text{O}_{8+\delta}$ crystals

D. Barnes,<sup>1,a)</sup> M. Sinvani,<sup>1</sup> A. Shaulov,<sup>1</sup> C. Trautmann,<sup>2</sup> T. Tamegai,<sup>3</sup> and Y. Yeshurun<sup>1</sup>

<sup>1</sup>Department of Physics, Center for High- $T_c$  Superconductivity and Institute for Nanotechnology and Advanced Materials, Bar-Ilan University, Ramat-Gan 52900, Israel

<sup>2</sup>Gesellschaft für Schwerionenforschung (GSI), Materialforschung Planckstr. 1, 64291 Darmstadt, Germany

<sup>3</sup>Department of Applied Physics, The University of Tokyo, Hongo, Bunkyo-ku, Tokyo 113-8656, Japan

(Presented 11 November 2008; received 15 September 2008; accepted 10 November 2008; published online 25 February 2009)

We report on generation of spatiotemporal oscillations of magnetic flux in a  $\text{Bi}_2\text{Sr}_2\text{CaCu}_2\text{O}_{8+\delta}$  crystal irradiated in part with 2.2 GeV Au ions. Flux oscillations are spontaneously excited after exposing the sample to a steady magnetic field near the order-disorder vortex phase transition line. The oscillations originate at the border between the irradiated and nonirradiated parts of the sample and propagate into the nonirradiated region toward the sample edge. Previously reported flux oscillations were observed in the vicinity of undefined defects in as grown  $\text{Bi}_2\text{Sr}_2\text{CaCu}_2\text{O}_{8+\delta}$  crystals. Observation of spontaneous oscillations in partially irradiated samples present the first attempt to generate such oscillations in a controlled manner. © 2009 American Institute of Physics. [DOI: 10.1063/1.3068647]

Magnetic relaxation in superconductors, due to thermally activated flux creep, has been the subject of wide basic and applied studies.<sup>1</sup> Recently, we reported on a new relaxation process associated with the annealing of transient disordered vortex states to the thermodynamically favored quasicrystalline phase.<sup>2,3</sup> These transient states, observed below the order-disorder transition induction  $B_{\text{od}}$  (Ref. 4) are inadvertently created by injection of vortices through inhomogeneous surface barriers.<sup>5</sup> Furthermore, we have shown that coupling between thermally activated flux creep and the annealing of transient disordered vortex states may produce spontaneous oscillations of vortex density in space and time.<sup>6,7</sup> These oscillations were observed in the vicinity of  $B_{\text{od}}$ , in proximity to an ill-defined defect, and were absent in clean samples lacking these defects. The present work describes the first attempt to generate such oscillations in a controlled manner. By introducing columnar defects<sup>8</sup> in part of a  $\text{Bi}_2\text{Sr}_2\text{CaCu}_2\text{O}_{8+\delta}$  (BSCCO) crystal, we were able to generate spatiotemporal flux oscillations, originating at the interface between the irradiated and unirradiated parts, by abruptly exposing the sample to a steady field just below  $B_{\text{od}}$ .

BSCCO single crystals ( $T_c=92$  K) grown by the floating zone method<sup>9</sup> were partially irradiated with 2.2 GeV Au ions at the linear accelerator Gesellschaft für Schwerionenforschung (GSI, Darmstadt, Germany). The irradiation was performed at room temperature and normal to the crystal surface ( $ab$  crystallographic plane). The range of the ions was larger than the sample thickness, i.e., the ions were not implanted into the crystal. During beam exposure, part of the sample was covered by a copper mask creating a sharp border between the irradiated and unirradiated parts of the sample (see Fig. 1). In this paper we present typical data, for a  $2.3 \times 0.93 \times 0.03$  mm<sup>3</sup> sample irradiated with a  $10^8$  ions/cm<sup>2</sup> fluence, corresponding to a matching field of

20 G (i.e., average defect distance of approximately 1  $\mu\text{m}$ ). Magneto-optical image sequences of the induction distribution were taken using an iron-garnet indicator with in-plane anisotropy<sup>10</sup> and a 12 bit Hamamatsu camera. In a typical magneto-optical measurement, the sample was zero-field-cooled to a target temperature between 20 and 30 K, and was then subjected to an external magnetic field applied parallel to the crystallographic  $c$ -axis of the crystal. The field was either applied abruptly ( $dH/dt > 3000$  Oe/s) to a constant value between 300 and 500 Oe or slowly ramped up at a rate of 7.5 Oe/s.

Figure 1(b) demonstrates the effect of the irradiation by showing a magneto-optical image of the sample in the remnant state after being exposed to a magnetic field of 700 G at 25 K. In this image, the brighter part indicates relatively large induction, i.e., stronger pinning due to irradiation. The sharp border between the irradiated and unirradiated parts is apparent.

Figure 2 shows induction profiles extracted from a magneto-optical sequence of images acquired while increasing the field at a rate of 7.5 Oe/s at 25 K. The time increment between profiles is 2 s (i.e., a change of 15 Oe in the external field). The unirradiated part (left of the dashed line) exhibits

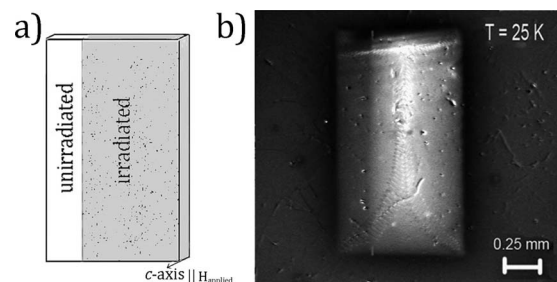


FIG. 1. (a) Schematic of the sample partly irradiated (gray area) by Au ions. External field is applied parallel to the crystallographic  $c$ -axis. (b) A Magneto-optical image of the sample in the remnant state at 25 K demonstrating the interface separating the two regions in the sample.

<sup>a)</sup>Author to whom correspondence should be addressed. Electronic mail: ph88@mail.biu.ac.il.

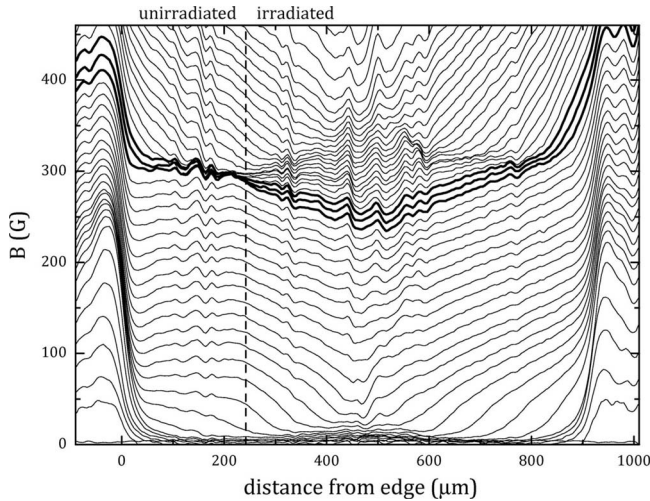


FIG. 2. Induction profiles measured at  $T=25$  K at time intervals of 2 s while the external field was ramped at a rate of 7.5 Oe/s. Dashed line marks the location of the border between the two regions. Bold profiles indicate the transition from dome to Bean profiles, which signifies the transition induction  $B_{od}$  in the unirradiated region. The static wiggles on the profiles are due to indicator imperfections and they do not change or move with time.

dome shaped profiles below inductions of 300 G, whereas the irradiated part exhibits Bean profiles at all inductions. The bold curves mark the transition from dome shape to Bean profiles in the unirradiated part, which indicate the induction  $B_{od}$  of the order-disorder transition.<sup>11</sup> In the irradiated part, at roughly the same inductions, a transition is observed from a relatively low  $j \propto dB/dx$  to a higher  $j$ . Thus, the partial irradiation creates two regions of qualitatively different flux distribution. Flux oscillations originate at the border between these regions when the induction is in the vicinity of  $B_{od}$ .

The spontaneous flux oscillations are demonstrated in Fig. 3, which shows the time evolution of the flux profiles at 25 K after an abrupt increase in the external field to a constant field of 460 Oe in less than 50 ms. The dashed line in the figure marks the location of the border between the two regions. Induction oscillations, originating at the border, are clearly observed in the unirradiated region. In the inset of Fig. 3 we zoom on a single oscillation as it propagates through the unirradiated region toward the edge of the sample. The profile exhibits a peak very close to the interface, indicating flux accumulation in this region and, as a result, the slope of the profile temporally inverted. The single cycle spans over 60  $\mu\text{m}$  over a period of 500 ms, yielding a spatial velocity of 120  $\mu\text{m/s}$ . It is important to note that the virgin sample, prior to irradiation, did not incorporate defects, which could result in flux oscillations as observed previously.<sup>6</sup> We also note that the magnetic relaxation at the irradiated region behaves monotonically and does not show any oscillations.

Figure 4 presents the temporal induction  $B(t)$  measured at 25 K with the external field applied abruptly to a constant value ranging from 340 to 485 Oe. The measured location on the sample is at the center of the unirradiated region, approximately 100  $\mu\text{m}$  from the irradiation border (indicated by an arrow in Fig. 3). The figure shows that induction oscillations are generated in a narrow

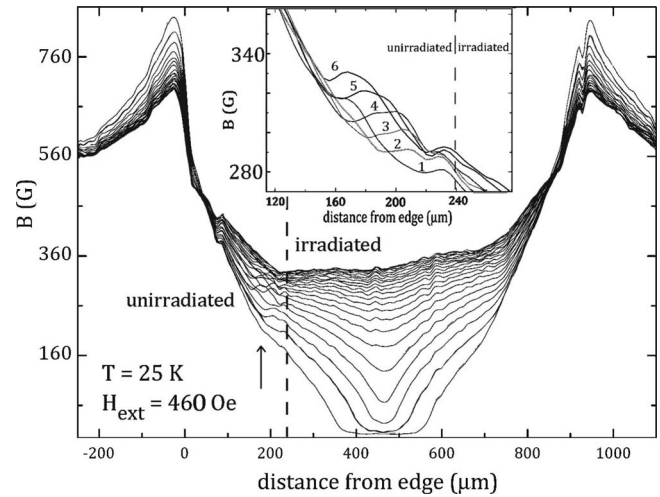


FIG. 3. Induction profiles across the entire sample at 25 K measured after field was applied abruptly to 460 Oe. Profiles are plotted in increments of 0.36 s between 0.8 and 8.5 s after application of the field. The dashed line marks the location of the border between the two regions. The arrow indicates the location at which the time sequence in Fig. 4 was taken. The zoomed curves in the inset demonstrate a single oscillation as it propagates with time toward the edge of the sample. The curves numbered 1 through 6 indicate profiles measured between  $t=1.8$  s and  $t=2.3$  s, respectively. Time interval between curves is 100 ms.

range of the external field between 400 and 500 Oe. For 485 Oe the oscillations are faster but have very small amplitude. The largest oscillation amplitude of roughly 40 G was measured for an applied field of 435 Oe. For observation of the full time evolution of the oscillatory induction profiles, the reader is referred to our website.<sup>12</sup>

Our experiments clearly show that the induction oscillations originate at the interface between the irradiated and unirradiated regions, where a discontinuity in the critical current density  $J_c$  and hence in the flux diffusivity  $D_f \propto 1/J_c$  occurs.<sup>13</sup> This observation is in accordance with our previous model for the origin of spontaneous flux oscillations.<sup>5,6,14</sup> According to this model, the oscillatory behavior of  $B$  with time at a certain location is associated with a periodic transformation of the vortex state, from quasicrystalline to disor-

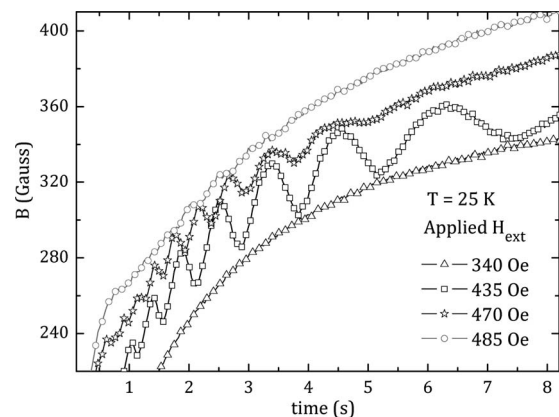


FIG. 4. Magnetic induction as a function of time measured after applying the external field abruptly to a constant value between 340 and 485 Oe at a temperature of 25 K. Measured location is at the unirradiated part of the sample approximately 100  $\mu\text{m}$  away from the irradiation border (indicated by an arrow in Fig. 3).

dered state and vice versa. In this transformation, two processes of magnetic relaxation, i.e., thermally activated flux creep and annealing of transient disordered vortex states, take place. Exposing the sample to an external field is followed by injection of a transient disordered vortex state into the sample. The annealing of this transient state is faster in the unirradiated region; consequently, nucleation of ordered state starts at the location of lowest induction in the unirradiated region, leading to a flat induction profile near the interface. Because of flux creep into the sample, the induction at the interface continues to increase. The discontinuity in the diffusion coefficient at the interface causes an accumulation of vortices at the interface up to a point where an inverted slope of  $B(x)$  is created. The inverted slope of  $B(x)$  reflects relatively high current density characteristic of a disordered vortex state. This inverted slope serves as a driving force for flux creep in the opposite direction, toward the sample edge. Consequently,  $B$  at the interface decreases and the vortex state there is ordered again. This process repeats itself, however, along with each cycle  $B$  increases and, as a result, the annealing process is becoming less and less effective, and therefore the oscillations eventually decay.

For the first time we artificially created conditions for generation of spontaneous flux oscillations in a superconductor. These oscillations are generated near the interface between irradiated and unirradiated parts of a BSCCO crystal. The ability to control the effect by creating artificial defects allows for more in-depth future studies of this phenomenon.

This research was supported in part by the Israel Science Foundation (ISF) Grant No. 499/07, and the Heinrich Hertz

Minerva Center for High Temperature Superconductivity. The authors would like to thank Daniel Levi for assistance in preparing the samples for the irradiation process and to Boris Ya. Shapiro and Baruch Rosenstein for valuable discussions.

- <sup>1</sup>Y. Yeshurun, A. P. Malozemoff, and A. Shaulov, *Rev. Mod. Phys.* **68**, 911 (1996).
- <sup>2</sup>D. Giller, A. Shaulov, T. Tamegai, and Y. Yeshurun, *Phys. Rev. Lett.* **84**, 3698 (2000).
- <sup>3</sup>B. Kalisky, Y. Bruckental, A. Shaulov, and Y. Yeshurun, *Phys. Rev. B* **68**, 224515 (2003).
- <sup>4</sup>E. Zeldov, A. I. Larkin, V. B. Geshkenbein, M. Konczykowski, D. Majer, B. Khaykovich, V. M. Vinokur, and H. Shtrikman, *Phys. Rev. Lett.* **73**, 1428 (1994).
- <sup>5</sup>Y. Paltiel, E. Zeldov, Y. Myasoedov, M. L. Rappaport, G. Jung, S. Bhattacharya, M. J. Higgins, Z. L. Xiao, E. Y. Andrei, P. L. Gammel, and D. J. Bishop, *Phys. Rev. Lett.* **85**, 3712 (2000).
- <sup>6</sup>B. Kalisky, M. Gitterman, B. Ya. Shapiro, I. Shapiro, A. Shaulov, T. Tamegai, and Y. Yeshurun, *Phys. Rev. Lett.* **98**, 017001 (2007).
- <sup>7</sup>D. Barness, I. Sochnikov, B. Kalisky, A. Shaulov, and Y. Yeshurun, *Physica C* **468**, 280 (2008).
- <sup>8</sup>L. Civale, A. D. Marwick, T. K. Worthington, M. A. Kirk, J. R. Thompson, L. Krusin-Elbaum, Y. Sun, J. R. Clem, and F. Holtzberg, *Phys. Rev. Lett.* **67**, 648 (1991).
- <sup>9</sup>N. Motohira, K. Kuwahara, T. Hasegawa, K. Kishio, and K. Kitazawa, *J. Ceram. Soc. Jpn.* **97**, 1009 (1989).
- <sup>10</sup>M. V. Indenbom, N. N. Kolesnikov, M. P. Kulakov, I. G. Naumenko, V. I. Nikitenko, A. A. Polyanskii, N. F. Vershinin, and V. K. Vlasko-Vlasov, *Physica C* **166**, 486 (1990).
- <sup>11</sup>D. Majer, E. Zeldov, H. Shtrikman, and M. Konczykowski, in *Coherence in High Temperature Superconductors*, edited by G. Deutscher and A. Revcolevschi (World Scientific, Singapore, 1996), pp. 271–296.
- <sup>12</sup>See <http://www.biu.ac.il/ESC/htslab/doron/index.htm>.
- <sup>13</sup>D. Barness, M. Sinvani, A. Shaulov, T. Tamegai, and Y. Yeshurun, *Phys. Rev. B* **77**, 094514 (2008).
- <sup>14</sup>M. Gitterman, B. Ya Shapiro, and I. Shapiro, *Europhys. Lett.* **76**, 1158 (2006).